RADIATION RESEARCH **165**, 721–729 (2006)
0033-7587/06 $15.00

Base Release in Nucleosides Induced by Low-Energy Electrons: A DFT Study

Xifeng Li,[a,1] Léon Sanche[a] and Michael D Sevilla[b,2]

[a] *Department of Nuclear Medicine and Radiobiology, Faculty of Medicine, Université de Sherbrooke, Quebec, J1H 5N4, Canada; and*
[b] *Department of Chemistry, Oakland University, Rochester, Michigan 48309*

Li, X., Sanche, L. and Sevilla, M.D Base Release in Nucleosides Induced by Low-Energy Electrons: A DFT Study. *Radiat. Res.* 165, 721–729 (2006).

Low-energy electrons are known to induce strand breaks and base damage in DNA and RNA through fragmentation of molecular bonding. Recently the glycosidic bond cleavage of nucleosides by low-energy electrons has been reported. These experimental results call for a theoretical investigation of the strength of the C_1'–N link in nucleosides (dA, dC and dT) between the base and deoxyribose before and after electron attachment. Through density functional theory (DFT) calculations, we compare the C_1'–N bond strength, i.e., the bond dissociation energy of the neutral and its anionic radical, and find that an excess electron effectively weakens the C_1'–N bond strength in nucleosides by 61–75 kcal/mol in the gas phase and 76–83 kcal/mol in the solvated environment. As a result, electron-induced fragmentation of the C_1'–N bond in the gas phase is exergonic for dA ($\Delta G = -14$ kcal/mol) and for dT ($\Delta G = -6$ kcal/mol) and is endergonic ($\Delta G = +1$ kcal/mol) only for dC. In the gas phase all the anionic nucleosides are found to be in valence states. Solvation is found to increase the exergonic nature by an additional 20 kcal, making the fragmentation both exothermic and exergonic for all nucleoside anion radicals. Thus C_1'–N bond breaking in nucleoside anion radicals is found to be thermodynamically favorable both in the gas phase and under solvation. The activation barrier for the C_1'–N bond breaking process was found to be about 20 kcal/mol in every case examined, suggesting that a 1 eV electron would induce spontaneous cleavage of the bond and that stabilized anion radicals on the DNA strand would undergo base release at only a modest rate at room temperature. These results suggest that base release from nucleosides and DNA is an expected consequence of low-energy electron-induced damage but that the high barrier would inhibit this process in the stable anion radicals. © 2006 by Radiation Research Society

INTRODUCTION

Ionizing radiation can cause serious damage to DNA, such as strand breaks and modification of it components (*1–3*). Ionizing radiation leaves a large number of secondary species along its track, including copious amounts of free electrons with kinetic energies below ~15 eV. In a dilute aqueous environment, the majority of these low-energy electrons will quickly thermalize and solvate (within $\sim 10^{-12}$ s) to become hydrated electrons (e_{aq}^-) that are unlikely to cause serious DNA damage (*1*). In highly concentrated aqueous solutions such as living tissues, direct ionization of local DNA components and attack of water radicals such as $^{\bullet}OH$ are considered to be responsible for most of the lethal DNA damage (*3*). The role of low-energy electrons in both direct DNA damage and radical production has not been yet elucidated. There is therefore a growing interest in assessing the contribution and enhancements of low-energy electron-induced fragmentation to the overall radiation damage processes.

The role of electrons with energies below the ionization energy threshold (~8 eV) in DNA damage was an open question until recently. The first definitive answer came from the work of Boudaiffa *et al.* (*4*), who reported clear evidence that low-energy electrons induce DNA strand breaks. This was followed by a series of experimental reports on low-energy electron-induced damages to DNA (*5–8*) and its components, including the deoxyribose moiety (*9, 10*), DNA and RNA bases (*11–18*), and nucleosides (*19–21*). In addition to these efforts, a number of theoretical studies have also been reported that investigated different aspects of the interactions of low-energy electrons with DNA or its components, such as strand breaks (*22–24*), modifications of the components (*25–27*), and the energetics of anion radicals (*28, 29*). The increasing list of reports has established the fact that low-energy electrons can be quite destructive through dissociative electron attachment (DEA) (*30*), the mechanism behind the fatal attachments (*31*) of low-energy electrons.

Our own theoretical explorations have covered a number of topics related to the interactions of low-energy electrons with DNA or its components, including strand breaks (*23*), hydrogen loss from bases (*25, 26*), radiosensitization (*25, 32*), and energetics (*33, 34*). There is also another area to explore theoretically, i.e., the glycosidic bond cleavage of nucleosides by low-energy electrons, reported recently (*19,*

[1] Current address: Patheon, Inc. 865 York Mills Road, Toronto, Ontario, Canada M3B 1Y5.
[2] Address for correspondence: Department of Chemistry, Oakland University, Rochester, Michigan 48309; e-mail: sevilla@oakland.edu.

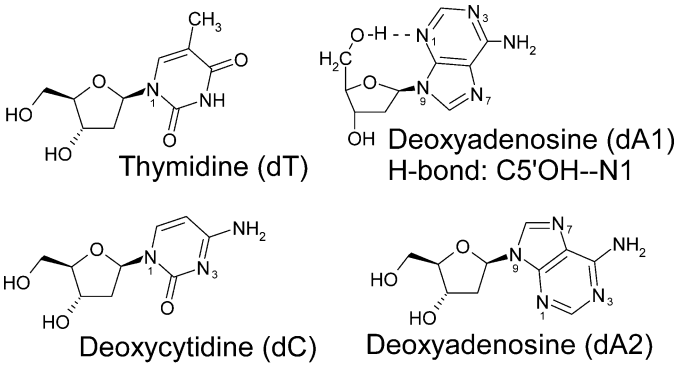

FIG. 1. Structures and names of the selected molecules. An internally H-bonded structure of dA is also included for illustrative purposes.

20). It has been found that 15 eV electrons can induce up to 10% of thymidine to be decomposed into thymine, which represents about one-third of the total low-energy electron-induced decomposition of thymidine; the initial quantum yield of conversion to thymine was estimated to be 3.2×10^{-2} per incident electron (*19*). It should be noted that electrons with lower energy (<3 eV) were also found to induce efficient dissociation of thymidine into the sugar and thymine moieties (*20*). Calculations show that the N_1–H is the weakest bond in thymine for cleavage by low-energy electrons (*27*). In our earlier work, we predicted that in nucleosides and even in DNA, the N_1 glycosidic bond to the deoxyribose would be a weak link and would be highly vulnerable to low-energy electron-induced bond fragmentation. Further, we note that radiation-induced base release is a well-known process that has been attributed to formation of sugar radicals followed by the loss of an unaltered base during chemical rearrangement (*35–38*). Recent results show that low-energy electrons should also induce unaltered base release so that DEA may also contribute to these yields. However, this prediction needs to be verified.

One theoretical report has addressed low-energy electron-induced base release for dT and dC (*39*). In the present work, we extend previous efforts to purine nucleosides and give detailed potential energy surfaces for the cleavage of the C_1'–N link in all nucleosides between the base and deoxyribose C1 before and after attachment of low-energy electrons. Structures of the nucleoside molecules, deoxycytidine (dC), deoxythymidine (dT, synonym: thymidine) and deoxyribose adenidine, both with (dA1) and without (dA2) internal H-bonding, are shown in Fig 1.

METHODS

All geometry optimizations, as well as the adiabatic potential energy surface searches, were performed in the gas phase using the DFT B3LYP functionals with the 6–31+G(d) basis set provided in the Gaussian 03 program (*40*). The B3LYP functional is a combination of exchange from Becke's three-parameter HF/DFT hybrid exchange functional (B3) with the dynamic correlation functional of Lee, Yang and Parr (LYP). For the accuracy of this level of theory, see ref. (*41*); for an in-depth discussion about the DFT functionals, see ref. (*42*).

The size and flexibility of any nucleoside molecule suggest that multiple stable configurations may exist for the neutral molecule and the corresponding anionic radical. It is not the purpose of the current work to explore such multiple possibilities, but rather to focus on the configuration as close as that within a natural DNA structure. Another consideration is to what degree the anionic radical shows a diffuse character in its singly occupied molecular orbital (SOMO). A calculation for valence states, which is the goal of this work, can be considered to fail if diffuse character contributes significantly (*33*). For example, we find that several anion radical configurations of dG show extensive diffuse character, although when an H-bond exists as in $C_5'OH$–N_1(G), a greater contribution of valence state is found. Because of the diffuse state mixing with the valence state, likely as a result of dG's low electron affinity, we do not report results for dG or 1-methyl thymine, which had a similar problem. Because their SOMOs and spin distributions show a dominant valence-state character, calculations reported in this work are focused on dT, dC and two structures of dA with and without internal $C_5'OH$–N_1 hydrogen bonding.

Adiabatic potential energy surfaces along the C1′–N bond stretch were calculated using optimization keyword opt=ModRedundant, with the S action code in the additional input, which performs geometry optimization for each point along the specified range of C_1'–N distances, from ~1 Å up to 3.0 Å. The optimized geometries found along the coordinates were verified further by frozen distance optimizations, which also served to obtain information about the charge/spin distributions and molecular orbital symmetry. Transition states were located by specifying opt=QST2 keyword, with the geometries of equilibrium anion and the dissociative state as input. These transition states are optimized and are confirmed to have only one imaginary frequency.

Using the optimized geometries, frequency calculations (without scaling) were performed at B3LYP with 6–31+G(d) basis set to obtain zero-point corrections to energy, the sum of electronic and thermal enthalpies (H), and the sum of electronic and thermal free energies (G). These values were used to calculate ''gas phase'' ΔH and ΔG for each reaction.

To obtain the energies under conditions of solvation (water), we chose the CPCM method and performed optimizations and frequency analysis at B3LYP/6–31+G(d) level, starting from the geometry optimized in the gas phase. The MO and spin density contours were visualized by g-OpenMol (*43*), using g03 check point files. The contour levels were ±0.01 for HOMO/LUMO and 0.0002 for spin density in e/au^3.

RESULTS AND DISCUSSION

C_1–N Bond Dissociation Energies before and after Electron Attachment

As an important indicator of a bond's strength, the neutral bond dissociation energy (nBDE) is defined as the energy needed for a homolytic bond dissociation:

$$\text{B-R} \rightarrow \text{B}^{\bullet} + \text{R}^{\bullet}, \qquad (1)$$

where B-R represents the neutral deoxynucleoside molecule, $B^{\bullet}$ is the base radical, and $R^{\bullet}$ is the deoxyribose C1 radical. Then the neutral bond dissociation energy of B-R bond is

$$\text{nBDE(B-R)} = \text{E}(\text{B}^{\bullet}) + \text{E}(\text{R}^{\bullet}) - \text{E(B-R)}. \qquad (2)$$

For radical anion, however, bond cleavage does not have a homolytic pathway as a result of the excess electron. Along the adiabatic pathway the final possession of the excess electron is decided by the electron affinities of the two fragmental radicals, and naturally the fragment with higher electron affinities gains the electron. As will be shown later,

TABLE 1
C1′–N Bond Dissociation Energies from Neutral Molecules and their Anion Radicals, Calculated at B3LYP/6-31+G(d) in kcal/mol and at 298 K

	Neutral bond dissociation energy: Base-R → Base• + R•			Anion radical bond dissociation energy: Base-R⁻ → Base⁻ + R•			Low-energy electron effect[c]
	nBDE[a]	ΔH	ΔG	aBDE[b]	ΔH	ΔG	nBDE − aBDE
Gas phase							
dT	71.22	71.81	56.41	7.08	7.68	−6.49	64.14
dC	75.91	76.50	61.59	14.88	15.47	0.86	61.03
dA1[d]	79.95	80.54	64.95	4.75	5.34	−8.81	75.20
dA2[d]	74.65	75.25	60.78	−0.48	0.11	−14.27	75.13
Solvated[e]							
dT	66.08	66.68	51.76	−9.93	−9.34	−24.18	76.01
dC	69.90	70.50	55.02	−7.35	−6.75	−21.86	77.25
dA1[d]	68.78	69.38	54.42	−10.25	−9.66	−24.81	79.03
dA2[d]	67.51	68.10	54.81	−15.96	−15.36	−28.56	83.47

[a] Zero point energy and thermal energy corrected.
[b] All anion radicals are in their valence states. See the Results for more discussion.
[c] The difference in the N–C_1' bond energy between the nucleoside neutral and anion radical is given by nBDE − aBDE. Note that nBDE − aBDE = EA (base radical fragment) − EA (nucleoside).
[d] With (dA1) and without (dA2) H-bonding $C_5'OHN_1$.
[e] Optimized using CPCM solvation model.

all the base radicals have higher electron affinities than the deoxyribose C1′ radical. Thus the C1′–N bond cleavage will proceed as shown in reaction (3),

$$B\text{-}R^{\bullet -} \rightarrow B^- + R^{\bullet}, \qquad (3)$$

where $B\text{-}R^{\bullet -}$ is the nucleoside anion radical, B^- is the base anion after cleavage, and $R^{\bullet}$ is the C1′ deoxyribose sugar radical fragment. We define the heterolytic anion bond dissociation energy (aBDE) as

$$aBDE(B\text{-}R^{\bullet -}) = E(B^-) + E(R^{\bullet}) - E(B\text{-}R^{\bullet -}). \qquad (4)$$

The changes in enthalpy and free energy can also be calculated in the same manner for bond cleavage in both neutral and anion radicals. We can further define the ''low-energy electron effect'' to be the difference between neutral bond dissociation energies and anion bond dissociation energy as a measure of the weakening effect of low-energy electron attachment. In effect, this is equivalent to the difference in the electron affinities of the base radical fragment and the original nucleoside.

Table 1 shows the bond dissociation energy, ΔH and ΔG for homolytic dissociation of the neutral C_1'–N bond and heterolytic dissociation of the anion, calculated for the sets of nucleosides. As can be seen, in the gas phase, all the bond dissociation energies of the neutral radicals are above 70 kcal/mol, with that of dA1 being highest, at 79.95 kcal/mol. Based on the neutral bond dissociation energies, the C_1'–N bonds strength, in the gas phase, are in the order dA1 > dA2 ≈ dC > dT. After an excess electron is added, the C_1'–N bond is significantly weakened, and the order of anionic bond dissociation energy becomes dC > dT > dA1 > dA2. In regard to the low-energy electron effect on bond strength (last column of Table 1), the greatest weakening effect is for dA (75 kcal/mol) and the least for dC (61 kcal/mol). For all anion radicals but the dC anion radical, the free energies (ΔG) of the heterolytic dissociation processes of the C_1'–N bonds are negative, indicating that these processes are intrinsically spontaneous in the gas phase. This is similar to the findings of Richardson *et al.* (*28*) on the ''hydrolysis'' of anionic nucleosides in the presence of water.

To estimate the influence of solvation, the gas-phase geometries were re-optimized under water solvation using the CPCM model. The calculated results of neutral and anionic bond dissociation energys are collected in the lower portion of Table 1. Solvation accounts for a decrease of about 6 (the pyrimidines) or 14 to 15 kcal/mol (for A) of the neutral nucleosides' bond dissociation energy, ΔH and ΔG. In contrast, the anions are far more sensitive to solvation than the neutrals radicals. Solvation leads to a decrease of about 17, 22 and 15 kcal/mol for dT, dC and dA, respectively, the bond dissociation energies, ΔHs and ΔEs of their anions, making each of these values negative. This is accounted for by the increased solvation energy of the more localized charge on the base fragment over the delocalized anion radical. This difference in the solvation effect on the neutral radical and its anion is also reflected in the 4 to 16-kcal/mol increase in the low-energy electron effect (the column for nBDE − aBDE) for the deoxynucleosides.

Internal H-bonding in dA1 between the $C_5'OH$ and N_1 increases the energy required to remove the base from the sugar fragments by about 5 kcal in the anion radicals compared to that found for dA2. This is a measure of the H-bond strength; the 5-kcal difference is also found in the neutral radicals without solvation. It is interesting to note that this H-bonding does not alter the low-energy electron

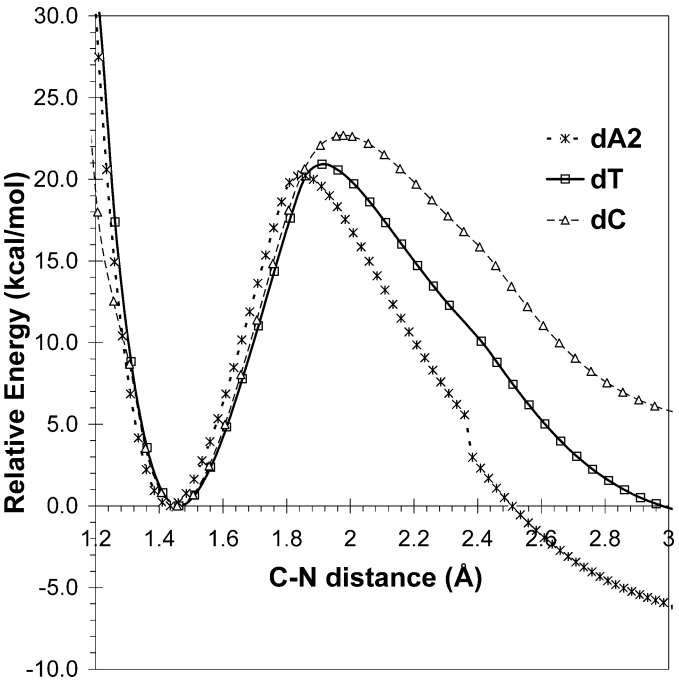

FIG. 2. Anionic N_1–C potential energy surfaces of deoxyribose adenine deoxyribose (dA2), thymine (dT: thymidine) and deoxyribose cytosine. dA1 has a similar profile to dA2.

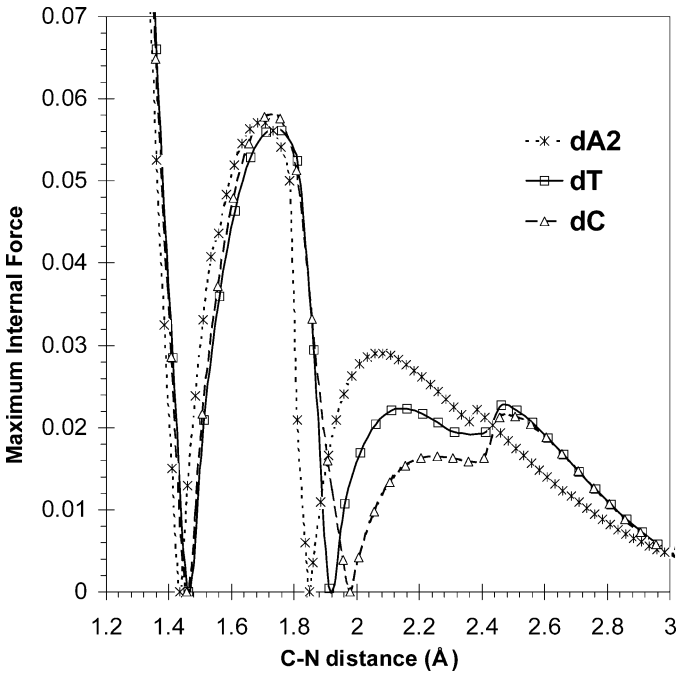

FIG. 3. The internal maximum force profiles as the N–C bond of dA1, dT or dC anion was stretched, calculated at B3LYP/6-31+G(d) level.

effect for dA. Under solvation, however, H-bonding in dA1 slightly reduces the low-energy electron effect.

These results clearly predict that a low-energy electron significantly weakens the C_1'–N links of a nucleoside between the deoxyribose and the base. Furthermore, an electron with excess kinetic energy greater than the activation barrier has the potential to induce bond cleavage. This is most likely for the purine nucleosides for which the bond cleavage is most exothermic.

One important implication of these results is that low-energy electrons may also induce base release from DNA. Clearly the glycosidic link to the purine base is predicted to be more susceptible to low-energy electron-induced fragmentation than the links to the pyrimidine bases (Table 1). It is well known from ESR experiments as well as theory that excess electrons energetically prefer to localize on the pyrimidine bases (thymine and cytosine) in DNA. Localization on the pyrimidine in DNA would decrease the possibility of a base release. However, a low-energy electron will interact favorably with an MO energy level in the DNA bases corresponding to its energy. This means that the LUMO of the DNA are not necessarily the most favored for electron capture. In fact, recent work on oligonucleotides by Naaman has shown that interactions with low-energy electrons are greater for those oligos containing guanine bases (*44*). On the other hand, within DNA, a low-energy electron that thermalizes and is captured has an extremely low probability of inducing thermal cleavage owing to the 20-kcal/mol activation barrier and the preferred localization to pyrimidine bases. Structural restrictions imposed by the DNA double-stranded structure such as caging effects within DNA will likely limit the bond cleavage further. Taking these into account, it is projected that low-energy electron-induced base release will be less efficient in DNA than from a single nucleoside.

The Potential Energy Surfaces and Profile of Maximum Internal Force

The bond dissociation energy of the neutral gives the thermodynamic energy difference for bond cleavage. However, the activation barrier is the rate-controlling factor, and we have estimated the activation barriers from our calculations of the potential energy surfaces, which give the energy change as a function of increasing bond distance.

Figure 2 shows the adiabatic potential energy surfaces on extension of the C_1'–N bonds of the dA2, dT and dC anions. At equilibrium, the C_1'–N bond distances of these three anions are all around 1.45 Å. As the C_1'–N bonds are

TABLE 2
Activation Energies in Gas Phase (kcal/mol) at B3LYP/6-31+G(d)

Transition state anion	$\Delta E^{\ddagger a}$	$\Delta H^{\ddagger b}$	$\Delta G^{\ddagger b}$	C_1'–N distance (Å)
dT	20.9	19.2	18.8	1.91
dC	22.7	20.8	20.1	1.98
dA1	20.3	19.1	19.2	1.85
dA2	19.5[c]	—	—	1.84

[a] Without ZPE corrections (optimized transition state).
[b] ZPE corrected (T = 298 K, optimized transition state).
[c] Estimated from potential energy surface.

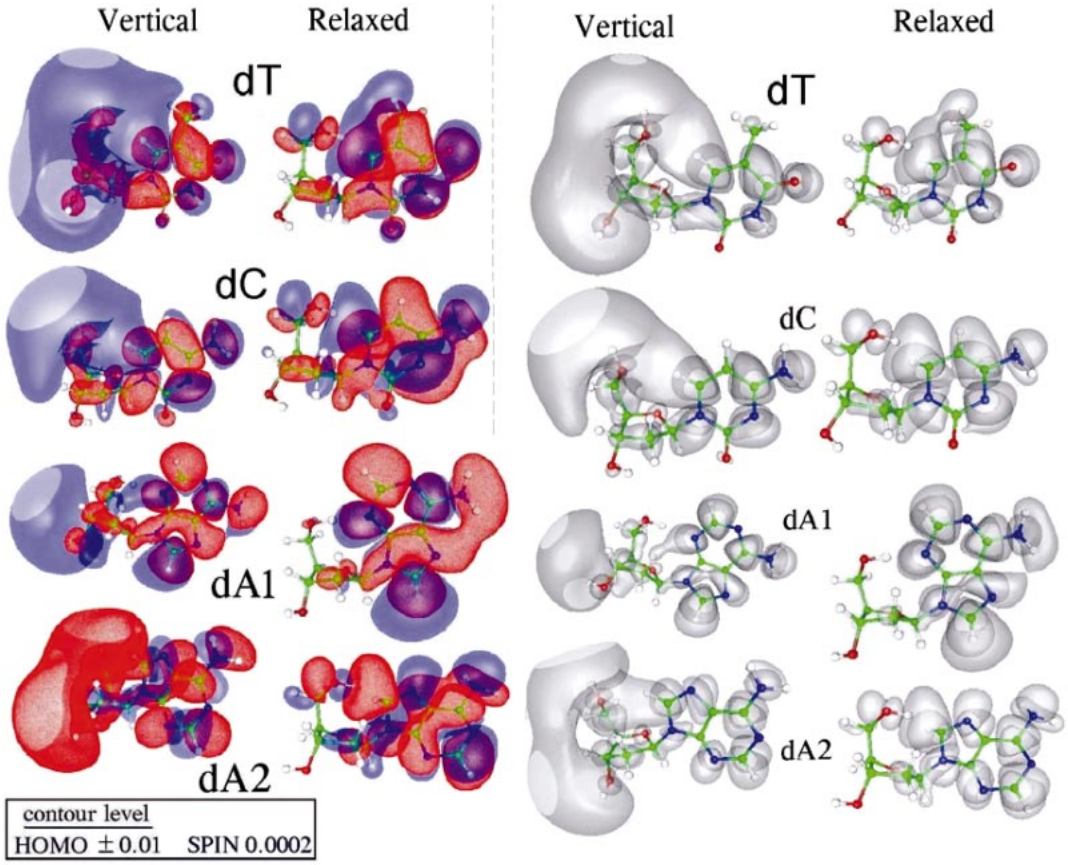

FIG. 4. SOMO (left, blue and red) and spin density (right, gray) contours of vertical and equilibrium anion radicals. Method: B3LYP/6-31+G(d). Note that the $C_5'OH$–N_1 H-bond exists in dA1.

stretched, the relative energies increase and reach the maxima at about 1.9 Å, then decrease as the bonds stretch further.

The profiles of maximum internal force of each anionic system as a function of the bond distance are shown in Fig 3. The maximum internal force is the absolute value of the slope at any point on the potential energy surfaces shown in Fig. 2 with the peaks corresponding to the steepest points on potential energy surfaces, while the minimum points of force correspond to either the equilibrium or transition states. Thus the force profile is a good indicator of geometry status and reveals internal geometry reorganization that does not show up as clearly in the potential energy surfaces. For example, the force profiles of dT reveal an interesting increase at about 2.4 Å that is not easily seen in the potential energy surfaces. An examination of its change in geometry shows that the deoxyribose radical fragment has the hydrogen on C_1' reoriented to the negatively charged N_1 of the thymine fragment. This small H-bonding interaction is gradually lost on extension of the C–N glycosidic bond.

The potential energy surfaces of dA2 is characterized by sharp maxima at around 1.85 Å, suggesting quick conversion from the π^* bonding to σ^* antibonding molecular states. Over the maximum in the potential energy surfaces of dA2, a smooth descent toward bond rupture is found. The potential energy surfaces of dA1 shows a nearly identical profile to dA2; thus internal H-bonding between $C_5'OH$ and N_1 does not significantly alter the energy profile for fragmentation of the C_1'–N bond.

The potential energy surfaces of dT, dC and dA1 are similar in that they all exhibit transitional maxima in the range between 1.8–2.0 Å, and then the energies decrease gradually with increasing bond distance (Fig. 2). Optimized transtion-state structures were found for dT, dC and dA1. The heights of the maxima, i.e. the activation energies, are found to be roughly 20 kcal/mol for dT, dC and dA1 and dA2 (Table 2). The activation energies for dT and dC are in good agreement with those reported by Gu *et al.* (*39*), who used a much larger basis set DZP++. The activation energies for dA2 were estimated to be 19.5 kcal/mol from its potential energy surface. In contrast to the report by Gu *et al.* (*39*), we did not find a strong interaction between H on O5′ and N_1(pyrimidine) in our transition states. In the pathway we investigated, the H(O5′)–N_1 distances in transition states are found to be 3.03 Å (dT), and 3.07 Å (dC). Significant H(O5′)–N_1 interactions are found to appear at C_1'–N distance beyond 2.4 Å, as shown in the internal force profiles (Fig. 2).

Recent experimental reports that show base release in thymidine (dT) for low-energy electrons of only 1 eV (23

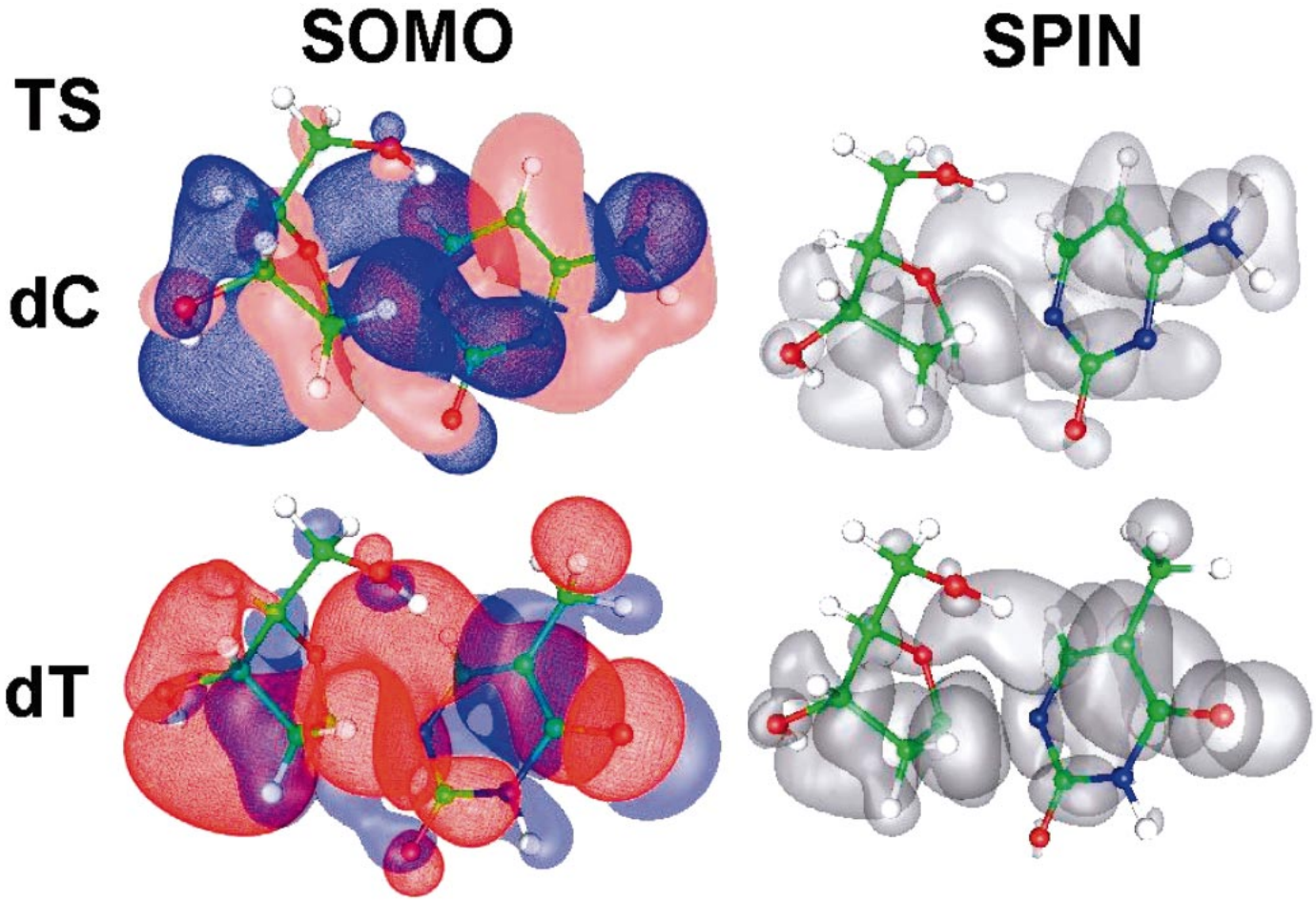

FIG. 5. SOMO (left, blue and red) and spin density (right, gray) contours of the dT and dC anion radicals at their respective optimized transition states. Method: B3LYP/6-31+G(d).

kcal) are in good agreement with the activation energy we have found (*19, 20*).

Distribution of Charge/Spin

Attachment of an excess electron to a neutral molecule inevitably alters the geometry of the molecule and affects the bond strengths within the molecule, particularly at sites of localization of the electron. Thus information about the charge and spin distributions of the resulting anion can help in understanding the effect of electron addition. The vertical anion radicals, i.e. anion radicals with the optimized neutral geometry, were used to check the charge/spin distributions after initial electron attachment but before geometrical relaxation occurs. This situation corresponds to the position of the nuclei when the electron is initially localized on the molecule (i.e., a vertical transition). Nuclear relaxation will occur after only picosecond residence times of the electron on the molecular framework; however, the bond fragmentation process will require longer residence times. The charge/spin information of the relaxed anions and for anion radicals along their C_1'–N potential energy surfaces are of our main interest as they are for valence states.

Figure 4 shows the SOMO/spin density contours of these anions both before and after relaxation. The HOMO and spin distribution contours of the vertical anions indicate that the electron has significant diffuse-state (unbound state) contributions mixed with the valence state for dC, dT and dA. In the limit of large basis sets, such electron distributions produce a free electron and the parent molecule or an electron dipole bound to the parent molecule. Thus these calculations can be considered to fail to describe the vertical valence anion state. However, after molecular relaxation, all these anions are in a valence π^* state in which the electron is delocalized in the π electron system on the DNA base. In Fig. 5 we show the SOMO and spin distribution calculated at the transition state for dT and dC. Here the spin is delocalized over the entire structure owing to the partial bonding nature in the transition state; however, the transition state is clearly a valence state. At long C_1'–N distances, the spin localizes on the C_1' sugar carbon and the charge is found largely at the free N_1 position on the base as expected.

Figure 6 shows the profile of total charge and spin on the base portion relative to the C_1'–N bond distance. As

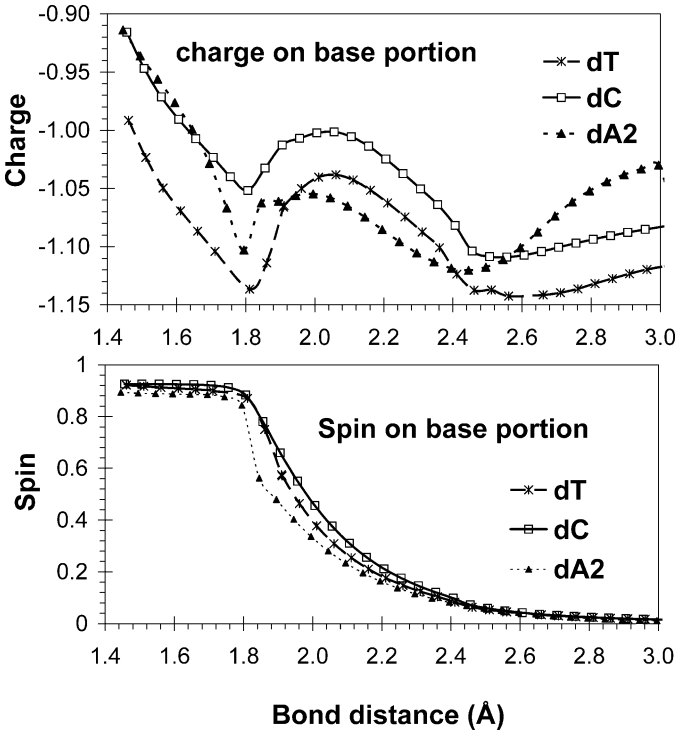

FIG. 6. Profile of charge and spin fraction on the base with C_1'–N bond stretching for anions of dT, dC and dA. Method: B3LYP/6-31+G(d).

the C_1'–N bond extends to 1.9 to 2.0 Å, the valence π^* state crosses the antibonding σ^* dissociative state. When the system crosses over to the σ^* dissociative state, the excess electron falls into the rupturing C_1'–N bond, creating a negative nitrogen site on the DNA base and a free radical at C_1' on the deoxyribose fragment. See the reaction below for thymidine radical anion:

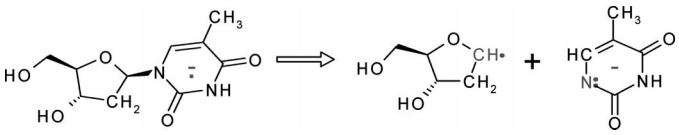

We note that the distributions of spin are as expected with the spin on the DNA base up to 1.8 Å and then, as the bond increases in length, the spin (but not the charge) transfers to the sugar fragment. One exception is found in the case of dA1, where we find a valence π^* anion at the start below 1.6 Å, but in the section between 1.6 and 1.8 Å the drop in spin on the base portion is found to reflect significant diffuse orbital mixing, not early rupture of the bond. For distances beyond 1.8 Å, a valence σ^* state is found. For nucleosides, these curves then are useful for keeping track of mixing of diffuse states for systems with electron affinities near zero.

Electron Affinities of all Species Involved

The electron affinities of the nucleosides and relevant fragments are important to the understanding of the damages of nucleosides induced by low-energy electrons and are reported in Table 3, which lists the adiabatic electron affinities of all molecules and the relevant fragments in the gas phase and in a solvated environment. For the relaxed molecular radical anions (geometry optimized), the SOMO and spin contours clearly indicate the character of a valence state (see Fig 4). The adiabatic electron affinities of the nucleosides are small: dT has the highest electron affinity (0.45 eV), and dA1 has the smallest valence adiabatic electron affinity (−0.038 eV) and is strongly affected by internal hydrogen bonding. In each of the equilibrium anionic nucleoside radicals (dA, dC, dT), the C_5'OH is pointing to the largest site of spin density on the base ring. This suggests that the electron is partially solvated and energetically stabilized by the nucleoside. Moreover, the electron affinity values suggest that the probability of thermal electron capture by any other nucleosides is highest for dT followed by dC. However, low-energy electron resonance capture occurs in unoccupied MOs within the entire secondary energy range of the low-energy electrons. Thus empty π^* bound states at 1 to 3 eV can capture electrons in this energy range and provide the mechanism for energy deposition and electron localization. This must be followed by crossing to a σ^* dissociative state, resulting in base release (*45*). Thus the largest positive adiabatic electron affinity may not be associated with the greatest likelihood of low-energy electron-induced dissociation.

Richardson *et al.* (*28*) reported the adiabatic electron affinities for dT (0.44), dC (0.33), dA (0.06) and dG (0.09

TABLE 3
Gas-Phase and Solvated Adiabatic Electron Affinities[a] of all Species Involved, Calculated at B3LYP/6-31+G(d) Level, (eV)

Molecule	Gas	Solvated[b]	Fragments	Gas	Solvated[b]
dT	0.45	1.90	Deoxyribose ($\cdot C_1'$)	0.50[c]	2.50
dC	0.33	1.81	$\cdot N_1$(T)	3.23	5.20
dA1[d]	−0.038	1.74	$\cdot N_1$(C)	2.97	5.16
dA2	−0.035	1.55	$\cdot N_9$(A)	3.22	5.17

[a] Adiabatic electron affinities are zero-point energy corrected and thermodynamically corrected to 298 K.
[b] In aqueous solvated environment, calculated using CPCM model.
[c] Internal H-bonding in C_1' anion: C_5'OH–O (sugar ring) = 1.99 Å.
[d] Internal H-bond between C_5'OH and N_1 (dA1).

eV), with all values being positive. There is excellent agreement between their values and ours for the pyrimidines (dT and dC; Table 3). However, their electron affinity value for dA is slightly higher. In the work of Richardson *et al.* (*28*), the optimized equilibrium anion of dA has an interesting H-bonding between H(sugar O5′) and C8 of adenine similar to that of dA2 in our work. While dA is a valence anion in the work of Richardson *et al.* (*28*), the dG anion shows an apparently diffuse character, and there is no internal H-bonding. Thus this state cannot be considered a valence anion.

In contrast, both the adiabatic and vertical electron affinities of the base radical fragments are over 2.5 eV and are all in localized valence states. The C_1' radical has an adiabatic electron affinity as high as 0.5 eV, which is due to the internal H-bonding between C_5'OH to the oxygen in the ring with a distance of 1.99 Å. Despite the contribution to electron affinity from the H-bonding, electron affinity of the C_1' radical is still less than any of the base fragments, leading to the excess electron being invariably localized to the base fragment, mainly at the nitrogen atom at the bond fragmentation site. In solution this site would be protonated quickly resulting in the free DNA base.

SUMMARY AND CONCLUSIONS

In experiments, it has been found that low-energy electrons can cause fragmentation at the C_1'–N link of nucleosides such as thymidine. This finding called for investigation of the strength of the C_1'–N bond in nucleosides before and after electron attachment as well as the energy profile of bond rupture reported here. We find that electron addition to a nucleoside yields a valence base anion radical and that this results in a reduction of the C_1'–N bond dissociation energies by over 70 kcal/mol. In fact, the anion radical bond dissociation energies are reduced to single digits or are actually negative in value. Under solvation, all the anionic bond dissociation energys become exothermic. Electron attachment quite effectively weakens the strength of the C_1'–N bond and promotes dissociation. The potential energy surface along the C_1'–N bond shows an activation barrier of about 20 kcal/mol for all nucleosides. As the C_1'–N bond is ruptured, the base fragment retains the charge because of its much higher electron affinity than the deoxyribose C_1' radical.

The 20-kcal/mol activation energies found in this work for bond cleavage leading to base release suggest slow reaction rates at room temperature from these adiabatic states. For example, if we assume a pre-exponential factor of 10^{13} in the simple relationship $k = Ae^{-Ea/kT}$, then at 300 K with our E_a of 20 kcal, the rate is predicted to be small, 3×10^{-2} s^{-1}. The known competitive reactions for the DNA base electron adducts are protonation at carbon sites (for example, at C_6 in dT and dC and at C_2 and C_8 for dG). These rates are far larger and range from 10^3 s^{-1} (dT, dC) to 10^4 s^{-1} (dG) (*46, 47*). As pointed out in this work, the expected route for the action of low-energy electron is not from the ground state but by resonant capture of the low-energy electron in metastable states above the activation barrier followed by crossing to the dissociative state (*45*).

ACKNOWLEDGMENTS

This research was supported by the Canadian Institutes of Health Research (CIHR), the National Cancer Institute of Canada and the NIH NCI Grant RO1CA045424, in joint efforts between the Faculty of Medicine of the Université de Sherbrooke and Department of Chemistry, Oakland University. Computer resources were provided, in part, by the Western Canada Research Grid (www.westgrid.ca).

Received: December 6, 2005; accepted: February 7, 2006

REFERENCES

1. C. von Sonntag, *The Chemical Basis for Radiation Biology*. Taylor & Francis, London, 1987.
2. D. Becker and M. D. Sevilla, The chemical consequences of radiation damage to DNA in *Adv. Radiat. Biol.* **17**, 121–180 (1993).
3. P. O'Neill, Radiation-induced damage in DNA. In *Radiation Chemistry,* pp. 585–622. Elsevier Science, Dordrecht, The Netherlands, 2001.
4. B. Boudaiffa, P. Cloutier, D. Hunting, M. A. Huels and L. Sanche, Resonant formation of DNA strand breaks by low-energy (3 to 20 eV) electrons. *Science* **287**, 1658–1660 (2000).
5. F. Martin, P. D. Burrow, Z. Cai, P. Cloutier, D. Hunting and L. Sanche, DNA strand breaks induced by 0–4 eV electrons: The role of shape resonances. *Phys. Rev. Lett.* **93**, 068101 (2004).
6. M. A. Huels, B. Boudaiffa, P. Cloutier, D. Hunting and L. Sanche, Single, double, and multiple double strand breaks induced in DNA by 3–100 eV electrons. *J. Am. Chem. Soc.* **125**, 4467–4477 (2003).
7. X. Pan, P. Cloutier, D. Hunting and L. Sanche, Dissociative electron attachment to DNA. *Phys. Rev. Lett.* **90**, 208102 (2003).
8. B. Boudaiffa, P. Cloutier, D. Hunting, M. A. Huels and L. Sanche, Cross sections for low-energy (10–50 eV) electron damage to DNA. *Radiat. Res.* **157**, 227–234 (2002).
9. S. Ptasinska, S. Denifl, P. Scheier and T. D. Märk, Inelastic electron interaction (attachment/ionization) with deoxyribose. *J. Chem. Phys.* **120**, 8505–8511 (2004).
10. D. Antic, L. Parenteau and L. Sanche, Electron-stimulated desorption of H^- from condensed-phase deoxyribose analogues: Dissociative electron attachment versus resonance decay into dipolar dissociation. *J. Phys. Chem. B* **104**, 4711–4716 (2000).
11. G. Hanel, B. Gstir, S. Denifl, P. Scheier, M. Probst, B. Farizon, M. Farizon, E. Illenberger and T. D. Märk, Electron attachment to uracil: Effective destruction at subexcitation energies. *Phys. Rev. Lett.*, **90**, 188104 (2003).
12. S. Denifl, S. Ptasinska, M. Probst, J. Hrusak, P. Scheier and T. D. Märk, Electron attachment to the gas-phase DNA bases cytosine and thymine. *J. Phys. Chem. A* **108**, 6562–6569 (2004).
13. S. Denifl, S. Ptasinska, M. Cingel, S. Matejcik, P. Scheier and T. D. Märk, Electron attachment to the DNA bases thymine and cytosine. *Chem. Phys. Lett.* **377**, 74–80 (2003).
14. A. M. Scheer, K. Aflatooni, G. A. Gallup and P. D. Burrow, Bond breaking and temporary anion states in uracil and halouracils: Implications for the DNA bases. *Phys. Rev. Lett.* **92**, 068102 (2004).
15. P. C. Dugal, H. Abdoul-Carime and L. Sanche, Mechanisms for low-energy (0.5–30 eV) electron-induced pyrimidine ring fragmentation within thymine- and halogen-substituted single strands of DNA. *J. Phys. Chem. B* **104**, 5610–5617 (2000).
16. M. A. Huels, I. Hahndorf, E. Illenberger and L. Sanche, Resonant dissociation of DNA bases by subionization electrons. *J. Chem. Phys.* **108**, 1309–1312 (1998).

17. R. Abouaf, J. Pommier and H. Dunet, Negative ions in thymine and 5-bromouracil produced by low energy electrons. *Int. J. Mass. Spectrom.* **226**, 397–403 (2003).

18. H. Abdoul-Carime, S. Gohlke and E. Illenberger, Site-specific dissociation of DNA bases by slow electrons at early stages of irradiation. *Phys. Rev. Lett.* **92**, 168103 (2004).

19. Y. Zheng, P. Cloutier, D. J. Hunting, J. R. Wagner and L. Sanche, Glycosidic bond cleavage of thymidine by low-energy electrons. *J. Am. Chem. Soc.* **126**, 1002–1003 (2004).

20. H. Abdoul-Carime, S. Gohlke, E. Fischbach, J. Scheike and E. Illenberger, Thymine excision from DNA by subexcitation electrons. *Chem. Phys. Lett.* **387**, 267–270 (2004).

21. H. Abdoul-Carime and L. Sanche, Sequence-specific damage induced by the impact of 3–30 eV electrons on oligonucleotides. *Radiat. Res.* **156**, 151–57 (2001).

22. R. Barrios, P. Skurski and J. Simons, Mechanism for damage to DNA by low-energy electrons. *J. Phys. Chem. B* **106**, 7991–7994 (2002).

23. X. Li, M. D. Sevilla and L. Sanche, DFT studies of electron interaction with DNA: Can zero eV electrons induce strand breaks? *J. Am. Chem. Soc.* **125**, 13668–13669 (2003).

24. J. Berdys, I. Anusiewicz, P. Skurski and J. Simons, Damage to model DNA fragments from very low-energy (<1 eV) electrons. *J. Am. Chem. Soc.* **126**, 6441–6447 (2004).

25. X. Li, M. D. Sevilla and L. Sanche, DFT investigation of dehalogenation of adenine-halouracil base pairs upon low energy electron attachment. *J. Am. Chem. Soc.* **125**, 8916–8920 (2003).

26. X. Li, L. Sanche and M. D. Sevilla, Low energy electron interactions with uracil: The energetics predicted by theory. *J. Phys. Chem. B* **108**, 5472–5476 (2004).

27. X. Li, M. D. Sevilla and L. Sanche, Hydrogen atom loss in pyrimidine DNA bases induced by low-energy electrons: Energetics predicted by theory. *J. Phys. Chem. B* **108**, 19013–19019 (2004).

28. N. Richardson, J. Gu, S. Wang, Y. Xie and H. F. Schaefer III, DNA nucleosides and their radical anions: Molecular structures and electron affinities. *J. Am. Chem. Soc.* **126**, 4404–4411 (2004).

29. O. Dolgounitcheva, V. G. Zakrzewski and J. V. Ortiz, Diffuse-bound and valence-bound anions of cytosine. *J. Phys. Chem. A* **105**, 8782–8786 (2001).

30. L. Sanche, Nanoscopic aspects of radiobiological damage: Fragmentation induced by secondary low-energy electrons. *Mass Spectr. Rev.* **21**, 349–369 (2002).

31. G. Collins, Fatal attachments: Extremely low energy electrons can wreck DNA. *Sci. Am.* **289**, 26–28 (2003).

32. X. Li, L. Sanche and M. D. Sevilla, Dehalogenation of 5-halouracils after low energy electron attachment: A density functional theory investigation. *J. Phys. Chem. A* **106**, 11248–11253 (2002).

33. X. Li, Z. Cai and M. D. Sevilla, Energetics of the radical ions of the AT and AU base pairs: A density functional theory (DFT) Study. *J. Phys. Chem. A* **106**, 9345–9351 (2002).

34. X. Li, Z. Cai and M. D. Sevilla, DFT calculations of the electron affinities of DNA/RNA bases: Dealing with negative electron affinities. *J. Phys. Chem. A* **106**, 1596–1603 (2002).

35. S. G. Swarts, M. D. Sevilla, D. Becker, C. J. Tokar and K. T. Wheeler, Radiation-induced DNA damage as a function of hydration. I. Release of unaltered bases. *Radiat. Res.* **129**, 333–344 (1992).

36. Y. Razskazovskiy, M. F. Debije and W. A. Bernhard, Direct radiation damage to crystalline DNA: What is the source of unaltered base release? *Radiat. Res.* **153**, 436–441 (2000).

37. E. S. Henle, R. Roots, W. R. Holley and A. Chatterjee, DNA strand breakage is correlated with unaltered base release after gamma-irradiation. *Radiat. Res.* **143**, 144–150 (1995).

38. J. R. Wagner, C. Decarroz, M. Berger and J. Cadet, Hydroxyl-radical-induced decomposition of 2′-deoxycytidine in aerated aqueous solutions. *J. Am. Chem. Soc.* **121**, 4101–4110 (1999).

39. J. Gu, Y. Xie and H. F. Schaefer, III, Glycosidic bond cleavage of pyrimidine nucleosides by low-energy electrons: A theoretical rationale. *J. Am. Chem. Soc.* **127**, 1053–1057 (2005).

40. *Gaussian 03*, Revision B.05. Gaussian, Inc., Pittsburgh, PA, 2003.

41. J. C. Rienstra-Kiracofe, G. S. Tschumper and H. F. Schaefer, III, Atomic and molecular electron affinities: Photoelectron experiments and theoretical computations. *Chem. Rev.* **102**, 231–282 (2002).

42. S. Andersson and M. Grüning, Performance of density functionals for calculating barrier heights of chemical reactions relevant to astrophysics. *J. Phys. Chem. A* **108**, 7621–7636 (2004).

43. openMol, version 3.00, 2005. [Available online at http://www.csc.fi/gopenmol]

44. S. G. Ray, S. S. Daub and R. Naaman, On the capturing of low-energy electrons by DNA. *Proc. Natl. Acad. Sci. USA* **102**, 15–19 (2005).

45. J. Berdys, P. Skurski and J. Simons, Damage to model DNA fragments by 0.25–1.0 eV electrons attached to a thymine π^* orbital. *J. Phys. Chem. B* **108**, 5800–5805 (2004).

46. C. Nese, Z. Yuan, M. N. Schuchman and C. Von Sonntag, Electron transfer from nucleobase electron adducts to 5-bromouracil. Is guanine an ultimate sink for the electron in irradiated DNA? *Int. J. Radiat. Biol.* **65**, 527–543 (1992).

47. L. P. Candeias and S. Steenken, Electron adducts of adenine nucleosides and nucleotides in aqueous-solution-protonation at 2 carbon sites (C2 and C8) and intramolecular and intermolecular catalysis by phosphate S. *J. Phys. Chem.* **96**, 937–944 (1992).